

## **PULSED BEAM EXPANSION OF ELECTROMAGNETIC APERTURE FIELDS**

**T. Melamed**

Department of Electrical and Computer Engineering  
Ben-Gurion University of the Negev, Beer Sheva 84105, Israel

**Abstract**—The present contribution is concerned with an exact frame-based pulsed-beams expansion of planar aperture time-dependent electromagnetic fields. The propagating field is described as a discrete superposition of tilted, shifted and delayed electromagnetic pulsed-beam waveobjects over the frame spectral lattice. Explicit asymptotic expressions for the electromagnetic pulsed-beam propagators are obtained for the commonly used pulsed-quadratic windows.

### **1. INTRODUCTION**

Beam-type field expansion schemes have been the subject of an intense research in the past decade for scalar time-harmonic [1–3] as well as time-dependent fields [4–7]. The motivation to use these expansions lies in their mutual spectral-spatial (and temporal for time-dependent fields) localization and the capability to propagate the expansions' waveobjects in different complex environments. Such scalar and electromagnetic (EM) wave solutions have been obtained in anisotropic medium [8–13], dispersive medium [14–17], inhomogeneous medium [18–22] and for inverse scattering [23–28]. Several *electromagnetic* beam scattering and diffraction problems have been solved for rough surface scattering [29,30], dielectric interfaces [31,32], stratified media [33–36], and more. The expansion propagating elements have been termed phase-space (spectral) Green's functions, as they link induced sources in the configuration-space to phase-space distributions of scattered fields, as well as phase-space distributions of incident fields to phase-space distributions of scattered fields [7,21]. Recently a novel beam-type waveobjects were obtained [22,37,38] by applying a non-orthogonal coordinate system

which is *a priori* matched to localized aperture field distributions. These waveobjects which were termed tilted Gaussian beams, are suitable for planar beam-type expansions and exhibit enhanced accuracy over the commonly used paraxial solutions.

An exact beam-type expansion of scalar planar aperture *time-dependent* fields was introduced in [4] for 2D and in [5] for 3D configurations in which the propagating fields are decomposed into a continuous spectrum of shifted, tilted and delayed pulsed-beam waveobjects. The *frame-based* field expansion utilizes the overcompleteness of phase-space representations and introduced a discrete spectral representation. This method for time-dependent fields was introduced in [6].

Though beam-expansion schemes for scalar fields have been the subject of intense research, electromagnetic expansions in terms of Gaussian/pulsed beams has been significantly less explored. In [39–41] Gaussian beams have been used for analysis of large reflector antennas, in which the expansion coefficients are obtained by numerically matching Gaussian beams to the far zone field of the feed antenna. These methods do not employ an *exact* field expansion schemes and therefore, they cannot be applied for near-field analysis, or in exact field calculations.

Recently the scalar time-harmonic field expansion scheme was extended to include *electromagnetic* fields in [42] where an exact frame-based expansion of planar aperture time-harmonic EM field was introduced. The propagating EM field was described as a discrete superposition of tilted and shifted EM Gaussian beams over the frame spectral lattice. The propagating waveobjects are localized solutions of Maxwell's equations which carry a Gaussian decay away from the beams' axes. In [43], an EM frame-based expansion was introduced in which the EM field was *a priori* decomposed into transverse electric and transverse magnetic wave polarizations by processing the transverse field components into novel TE and TM EM beam-type waveobjects. The present investigation extends the time-harmonic representation in [42] for time-dependent EM aperture fields and introduces the time-dependent EM pulsed-beam waveobjects which are requires for the exact expansion as well as their asymptotic evaluation.

## 2. PLANE-WAVE DECOMPOSITION

We are concerned with obtaining a discrete exact pulsed-beam spectral representation for the time-dependent EM field in  $z \geq 0$  due to sources in  $z < 0$ , given the transverse electric field components over  $z = 0$

plane

$$\mathbf{E}_0(\mathbf{r}_t, t) = E_x(\mathbf{r}_t, t)\hat{\mathbf{x}} + E_y(\mathbf{r}_t, t)\hat{\mathbf{y}}, \quad (1)$$

where  $\hat{\mathbf{x}}$  and  $\hat{\mathbf{y}}$  are the conventional cartesian unit-vectors and  $\mathbf{r}_t = (x, y)$  denotes the *transverse* coordinates. We use the conventional cartesian coordinate system in which the configuration space is described by  $\mathbf{r} = (x, y, z)$ . Here and henceforth hat over vector denotes a unit vector. The propagation medium is homogeneous with  $\epsilon_0$  and  $\mu_0$  denoting the free space permittivity and permeability, respectively.

### 2.1. Analytic Fields

In order to gain flexibility in the derivation, particularly when evanescent spectra are involved, it is convenient to use the analytic field representation. Given a real field  $\mathbf{E}(\mathbf{r}, t)$  that is defined for real (physical) time  $t$ , the corresponding analytic field is defined by the convolution integral

$$\breve{\mathbf{E}}(\mathbf{r}, t) = \frac{-1}{\pi j} \int_{-\infty}^{\infty} dt' \frac{\mathbf{E}(\mathbf{r}, t')}{t - t'}, \quad \text{Im}t \geq 0. \quad (2)$$

Here and henceforth, analytic fields are denoted by a breve mark ( $\breve{\cdot}$ ). Note that though the physical time is real, the *time argument* of an analytic field can be complex (see for example Eq. (9)). The limit of the analytic field on the *real*  $t$ -axis is related to the *real* field  $\mathbf{E}(\mathbf{r}, t)$  by

$$\breve{\mathbf{E}}(\mathbf{r}, t) = \mathbf{E}(\mathbf{r}, t) - j\mathcal{H}_t\mathbf{E}(\mathbf{r}, t), \quad t \text{ real} \quad (3)$$

where  $\mathcal{H}_t = \mathcal{P}(1/\pi t) \otimes$  is the Hilbert transform operator, with  $\mathcal{P}$  denoting Cauchy's principal value and  $\otimes$  denoting a temporal convolution. Therefore the real field for real  $t$  is recovered from the analytic field via

$$\mathbf{E}(\mathbf{r}, t) = \text{Re}\breve{\mathbf{E}}(\mathbf{r}, t). \quad (4)$$

Alternatively the analytic field  $\breve{\mathbf{E}}(\mathbf{r}, t)$  can be obtained by applying a one-sided (positive frequencies) inverse Fourier transform to the spectral (frequency domain) distribution of the real field  $\mathbf{E}(\mathbf{r}, t)$ . Since this paper is concerned with a *direct* time-domain derivation this approach is not investigated here.

### 2.2. Transient Plane-wave Representation

The analytic transient plane-wave spectral distribution,  $\breve{\mathbf{E}}_0(\boldsymbol{\kappa}_t, \tau)$  of the time-dependent aperture field over the  $z = 0$  plane,  $\mathbf{E}_0(\mathbf{r}_t, t)$ , is defined by [44]

$$\breve{\mathbf{E}}_0(\boldsymbol{\kappa}_t, \tau) = \int d^2x \breve{\mathbf{E}}_0(\mathbf{r}_t, \tau + c^{-1}\boldsymbol{\kappa}_t \cdot \mathbf{r}_t), \quad (5)$$

where  $\boldsymbol{\kappa}_t = (\kappa_x, \kappa_y)$  are the directional spectral variables,  $\tau$  denotes the temporal spectral variable and  $c$  denotes the speed of light in vacuo. Eq. (5) is a Radon transform of  $\check{\mathbf{E}}_0(\mathbf{r}_t, t)$  in the three dimensional  $(\mathbf{r}_t, t)$  space, consisting of projections of  $\check{\mathbf{E}}_0(\mathbf{r}_t, t)$  along surfaces of linear delay. It extracts from  $\check{\mathbf{E}}_0(\mathbf{r}_t, t)$  the transient plane-wave field which is propagating in a  $\boldsymbol{\kappa}_t$ -dependent direction (see (9)).

The inverse transform is of (5) is given by

$$\check{\mathbf{E}}_0(\mathbf{r}_t, t) = \frac{-1}{(2\pi c)^2} \int d^2 \kappa_t \partial_t^2 \check{\mathbf{E}}_0(\boldsymbol{\kappa}_t, t - c^{-1} \boldsymbol{\kappa}_t \cdot \mathbf{r}_t), \quad (6)$$

where  $\partial_t^2 = \partial^2 / \partial t^2$ . The aperture field distribution in (6) can easily be propagated into  $z > 0$  half-space by applying a standard plane-wave analysis. The longitudinal spectral component in the  $z$  direction is obtained from Gauss law

$$\check{E}_z(\boldsymbol{\kappa}_t, \tau) = -(\kappa_x \check{E}_x + \kappa_y \check{E}_y) / \kappa_z, \quad (7)$$

where

$$\kappa_z = \sqrt{1 - \kappa_x^2 - \kappa_y^2}, \quad \text{Re} \kappa_z \geq 0, \quad \text{Im} \kappa_z \leq 0. \quad (8)$$

Thus the electric field in  $z \geq 0$  is given by the plane-wave superposition

$$\check{\mathbf{E}}(\mathbf{r}, t) = \frac{-1}{(2\pi c)^2} \int d^2 \kappa_t \partial_t^2 \check{\mathbf{E}}(\boldsymbol{\kappa}_t, t - c^{-1} \hat{\boldsymbol{\kappa}} \cdot \mathbf{r}), \quad (9)$$

where

$$\check{\mathbf{E}}(\boldsymbol{\kappa}_t, \tau) = \check{\mathbf{E}}_0(\boldsymbol{\kappa}_t, \tau) + \hat{\mathbf{z}} \check{E}_z(\boldsymbol{\kappa}_t, \tau), \quad (10)$$

and the unit vector

$$\hat{\boldsymbol{\kappa}} = (\kappa_x, \kappa_y, \kappa_z). \quad (11)$$

The transient plane-wave representation in (9) describes the electric field  $\check{\mathbf{E}}(\mathbf{r}, t)$  in term of an angular superposition of transient EM plane-wave propagators each emanates from  $z = 0$  plane in the direction of the unit-vector  $\hat{\boldsymbol{\kappa}}$  in (11).

### 3. SCALAR FRAME-BASED PULSED-BEAM EXPANSION

In order to establish the EM frame-based pulsed-beam expansion we shall briefly review here the main results of the *scalar* time-dependent frame-based beam decomposition which was introduced in [6]. Time-dependent beam summation is constructed in the framework of the windowed Radon transform frames, where the aperture field  $\check{u}_0(\mathbf{r}_t, t)$  is expanded using a set of windowed Radon transform functions. The

aperture field  $\check{u}_0(\mathbf{r}_t, t)$  is assumed to be band-limited in the frequency interval

$$\Omega = (\omega_{\min}, \omega_{\max}). \tag{12}$$

The pulsed-beam expansion is constructed over the discrete 5D frame spectral lattice

$$(\bar{x}, \bar{y}, \bar{\kappa}_x, \bar{\kappa}_y, \bar{\tau}) = (N_x \Delta \bar{x}, N_y \Delta \bar{y}, N_{\kappa_x} \Delta \bar{\kappa}_x, N_{\kappa_y} \Delta \bar{\kappa}_y, N_\tau \Delta \bar{\tau}), \tag{13}$$

where  $(\Delta \bar{x}, \Delta \bar{y})$  are the unit-cell dimensions in the  $(x, y)$  coordinates, and  $(\Delta \bar{\kappa}_x, \Delta \bar{\kappa}_y)$  and  $\Delta \bar{\tau}$  denote the unit-cells dimensions in the spectral variables  $(\kappa_x, \kappa_y)$  and  $\tau$ , respectively. We use the index  $\mathbf{N} = (N_x, N_y, N_{\kappa_x}, N_{\kappa_y}, N_\tau)$  to tag the lattice points (see Figure 1). These unit-cell dimensions satisfy

$$\Delta \bar{x} \Delta \bar{\kappa}_x = 2\pi\nu_x, \quad \Delta \bar{y} \Delta \bar{\kappa}_y = 2\pi\nu_y, \quad \Delta \bar{\tau} < \pi/\omega_{\max}, \tag{14}$$

where  $0 \leq \nu_{x,y} \leq 1$  are the overcompleteness (or oversampling) parameters in  $x$  and  $y$  axes, respectively. The lattice is overcomplete for  $\nu_{x,y} < 1$ , critically complete in the Gabor limit  $\nu_{x,y} \uparrow 1$  [45], and for  $\nu_{x,y} \downarrow 0$  the discrete parametrization attains the continuity limit as in [4, 5]. It is convenient to chose equal-direction unit-cell dimensions  $\Delta \bar{\kappa}_x = \Delta \bar{\kappa}_y = \Delta \bar{\kappa}$  and equal-space unit-cell dimensions  $\Delta \bar{x} = \Delta \bar{y} = \Delta \bar{r}_t$ , though this choice is not essential. The unit cell dimensions should satisfy the overcompleteness criterion

$$\frac{\bar{\omega}}{c} \Delta \bar{\kappa} \Delta \bar{r}_t = 2\pi\nu, \tag{15}$$

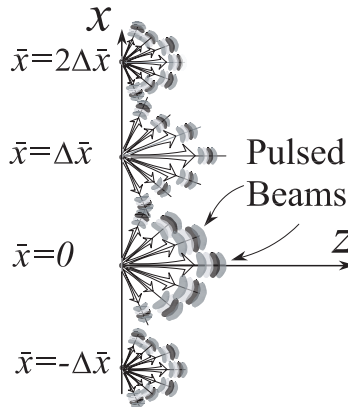


**Figure 1.** Discrete frame spectral lattice. The fields in  $z \geq 0$  are evaluated by superposition of tiled, shifted and delayed pulsed-beams which are emanating from the aperture distribution plane over the discrete frame spatial-directional-temporal lattice in (13).

at some reference frequency  $\bar{\omega}$ , that is chosen to be greater than  $\omega_{\max}$ , i.e.,  $\bar{\omega} = A\omega_{\max}$  with typically  $2.5 < A < 3$  [6]. In (15),  $0 \leq \nu \leq 1$  is termed the overcompleteness parameter.

After constructing the frame spectral lattice a proper synthesis (“mother”) window which is denoted by  $\check{\psi}(\mathbf{r}_t, t)$  is chosen. The frame representation of some aperture scalar field distribution over  $z = 0$  plane is given by

$$u_0(\mathbf{r}_t, t) = \sum_N a^N \psi^N(\mathbf{r}_t, t), \quad (16)$$

where the expansion frame-set,  $\psi^N(\mathbf{r}_t, t)$ , are obtained from the synthesis window  $\psi(\mathbf{r}_t, t)$  via

$$\psi^N(\mathbf{r}_t, t) = \psi[\mathbf{r}_t - \bar{\mathbf{r}}_t, t - \bar{t} - c^{-1}\bar{\boldsymbol{\kappa}}_t \cdot (\mathbf{r}_t - \bar{\mathbf{r}}_t)]. \quad (17)$$

Throughout the paper superscript  $N$  denotes an object over the frame spectral lattice in (13). In the frame representation in (16), the expansion coefficients  $a^N$  are given by the inner product of the aperture field with the so-called analysis (“dual”) window,  $\varphi(\mathbf{r}_t, t)$ , namely,

$$a^N = \int d^2\mathbf{r}_t \int du_0(\mathbf{r}_t, t) \varphi^N(\mathbf{r}_t, t), \quad (18)$$

where

$$\varphi^N(\mathbf{r}_t, t) = \varphi[\mathbf{r}_t - \bar{\mathbf{r}}_t, t - \bar{t} - c^{-1}\bar{\boldsymbol{\kappa}}_t \cdot (\mathbf{r}_t - \bar{\mathbf{r}}_t)]. \quad (19)$$

The analysis window can be evaluated by several ways which are listed in [6] (see also (37)). Eq. (16) represents the aperture field as a discrete superposition of shifted, tilted and delayed time-dependent windows, each are localized about the frame lattice points which are tagged by the index  $N$ .

The scalar field in  $z > 0$  due to sources in  $z < 0$  is obtained by propagating each  $\psi^N(\mathbf{r}_t, t)$  window element in summation (16) into  $z > 0$  half-space. Therefore, the frame-based representation of the field in  $z \geq 0$  is given by

$$u(\mathbf{r}, t) = \sum_N a^N P^N(\mathbf{r}, t), \quad (20)$$

where each beam propagator,  $P^N$ , satisfies the scalar wave equation

$$[\nabla^2 - c^{-2}\partial_t^2] P^N(\mathbf{r}, t) = 0, \quad (21)$$

subject to causality boundary conditions. The beam propagator can be evaluated in several ways such as time-dependent Green’s function (Kirchhoff’s) integration or by applying a transient plane-wave spectral decomposition of the form in (9), i.e.,  $P^N(\mathbf{r}, t) = \text{Re}\check{P}^N(\mathbf{r}, t)$  where

$$\check{P}^N(\mathbf{r}, t) = \frac{-1}{(2\pi c)^2} \int d^2\boldsymbol{\kappa}_t \partial_t^2 \check{\psi}^N(\boldsymbol{\kappa}_t, t - c^{-1}\hat{\boldsymbol{\kappa}} \cdot \mathbf{r}), \quad (22)$$

with  $\check{\check{\psi}}^N$  denoting the transient plane-wave spectrum (5) of  $\check{\psi}^N(\mathbf{r}_t, t)$

$$\check{\check{\psi}}^N(\boldsymbol{\kappa}_t, \tau) = \int d^2x \check{\psi}^N(\mathbf{r}_t, \tau + c^{-1}\boldsymbol{\kappa}_t \cdot \mathbf{r}_t). \quad (23)$$

By inserting (17) into (23), we identify

$$\check{\check{\psi}}^N(\boldsymbol{\kappa}_t, \tau) = \check{\psi}(\boldsymbol{\kappa}_t - \bar{\boldsymbol{\kappa}}_t, \tau - \bar{\tau} + c^{-1}\boldsymbol{\kappa}_t \cdot \bar{\mathbf{r}}_t). \quad (24)$$

The spectral representation in (20) describes the field as a discrete superposition of pulse-beam waveobjects, that emanate from points  $(\bar{x}, \bar{y})$  on the frame spectral lattice, in a discrete set of directions which are determine by the spectral wavenumbers  $(\bar{\kappa}_x, \bar{\kappa}_y)$  and in a discrete set of delays  $\bar{\tau}$  (see Figure 1). In order to obtain a discrete EM *vectorial* frame-based representation, we find a frame spectral representation for the transient plane-wave spectrum of the aperture field,  $\check{\check{u}}_0(\boldsymbol{\kappa}_t, \tau)$ . By applying the Radon transform operator in (23) to the analytic continuation of (16),  $\check{u}_0(\mathbf{r}_t, t)$ , and inverting the order of integration and summation we obtain

$$\check{\check{u}}_0(\boldsymbol{\kappa}_t, \tau) = \sum_N a^N \check{\check{\psi}}^N(\boldsymbol{\kappa}_t, \tau), \quad (25)$$

where  $\check{\check{\psi}}^N$  is given in (24) and the expansion coefficients are evaluated from the aperture field via (18).

#### 4. ELECTROMAGNETIC PULSED-BEAM EXPANSION

In order to obtain a frame-based representation of the transient electric field,  $\mathbf{E}(\mathbf{r}, t)$ , we define the coefficients vector  $\mathbf{a}^N$  via the inner product

$$\mathbf{a}^N = a_x^N \hat{\mathbf{x}} + a_y^N \hat{\mathbf{y}} = \int d^2r_t dt \mathbf{E}_0(\mathbf{r}_t, t) \varphi^N(\mathbf{r}_t, t), \quad (26)$$

where the analysis window  $\varphi^N(\mathbf{r}_t, t)$  is given in (19). Using (25) for each electric field transverse component, we may write

$$\check{\check{\mathbf{E}}}_0(\boldsymbol{\kappa}_t, \tau) = \sum_N \mathbf{a}^N \check{\check{\psi}}^N(\boldsymbol{\kappa}_t, \tau), \quad (27)$$

where  $\check{\check{\psi}}^N(\boldsymbol{\kappa}_t, \tau)$  is given in (24). By inserting (27) with (7) into (9) and inverting the order of integration and summation, we obtain

$$\check{\check{\mathbf{E}}}(\mathbf{r}, t) = \sum_N \frac{1}{(2\pi)^2} \int d^2\kappa_t [a_x^N \tilde{\mathbf{T}}_x + a_y^N \tilde{\mathbf{T}}_y] \partial_t^2 \check{\check{\psi}}^N(\boldsymbol{\kappa}_t, t - c^{-1}\hat{\boldsymbol{\kappa}} \cdot \mathbf{r}), \quad (28)$$

where  $a_x^N$  and  $a_y^N$  are given in (26), and

$$\tilde{\mathbf{T}}_x(\boldsymbol{\kappa}_t) = \hat{\mathbf{x}} - \kappa_z^{-1} \kappa_x \hat{\mathbf{z}}, \quad \tilde{\mathbf{T}}_y(\boldsymbol{\kappa}_t) = \hat{\mathbf{y}} - \kappa_z^{-1} \kappa_y \hat{\mathbf{z}}. \quad (29)$$

By using  $-c\partial_x\check{\psi}^N(\boldsymbol{\kappa}_t, t - c^{-1}\hat{\boldsymbol{\kappa}} \cdot \mathbf{r}) = \kappa_x\partial_t\check{\psi}^N(\boldsymbol{\kappa}_t, t - c^{-1}\hat{\boldsymbol{\kappa}} \cdot \mathbf{r})$ , and so forth, the real part of (28) yields

$$\mathbf{E}(\mathbf{r}, t) = \sum_N a_x^N \mathbf{E}_x^N(\mathbf{r}, t) + a_y^N \mathbf{E}_y^N(\mathbf{r}, t), \quad (30)$$

where the electric fields of the *EM beam propagators*,  $\mathbf{E}_x^N(\mathbf{r}, t)$  and  $\mathbf{E}_y^N(\mathbf{r}, t)$ , are obtained from the *scalar beam propagator*

$$P^N(\mathbf{r}, t) = \text{Re} \frac{1}{(2\pi c)^2} \int d^2\kappa_t \kappa_z^{-1} \partial_t \check{\psi}^N(\boldsymbol{\kappa}_t, t - c^{-1}\hat{\boldsymbol{\kappa}} \cdot \mathbf{r}), \quad (31)$$

via

$$\begin{aligned} \mathbf{E}_x^N(\mathbf{r}, t) &= -c(\hat{\mathbf{x}}\partial_z - \hat{\mathbf{z}}\partial_x)P^N(\mathbf{r}, t), \\ \mathbf{E}_y^N(\mathbf{r}, t) &= -c(\hat{\mathbf{y}}\partial_z - \hat{\mathbf{z}}\partial_y)P^N(\mathbf{r}, t). \end{aligned} \quad (32)$$

Equation (30) with (31) and (32) represent the electric field,  $\mathbf{E}(\mathbf{r}, t)$ , as a discrete superposition of EM pulsed-beam waveobjects,  $\mathbf{E}_x^N$  and  $\mathbf{E}_y^N$ , which are the electric field propagators due to the aperture electric field  $x$  and  $y$  components over  $z = 0$  plane, respectively. The excitation amplitudes of these EM waveobjects,  $a_x^N$  and  $a_y^N$ , are obtained by projecting the aperture field distribution on the analysis window as in (26). The spectral summation in (30) represents the electric field in terms of a discrete superposition of localized EM pulsed-beam propagators which emanate from each point over the frame spectral lattice in (13). The beam propagators are characterized by spatial and temporal localization and high directivity (see specific example for pulsed-quadratic windows in (48)–(51)).

By applying Faraday's law,  $\partial_t \mathbf{H} = -\mu_0^{-1} \nabla \times \mathbf{E}$ , to (30), we obtain the corresponding magnetic field in  $z \geq 0$

$$\mathbf{H}(\mathbf{r}, t) = \sum_N a_x^N \mathbf{H}_x^N(\mathbf{r}, t) + a_y^N \mathbf{H}_y^N(\mathbf{r}, t), \quad (33)$$

where the magnetic fields of the *EM beam propagators*,  $\mathbf{H}_x^N$  and  $\mathbf{H}_y^N$ , are given by

$$\begin{aligned} \mathbf{H}_x^N(\mathbf{r}, t) &= \frac{c}{\mu_0} [\hat{\mathbf{x}}\partial_{xy}^2 - \hat{\mathbf{y}}(\partial_x^2 + \partial_z^2) + \hat{\mathbf{z}}\partial_{yz}^2] P^N(\mathbf{r}, t), \\ \mathbf{H}_y^N(\mathbf{r}, t) &= \frac{c}{\mu_0} [\hat{\mathbf{x}}(\partial_y^2 + \partial_z^2) - \hat{\mathbf{y}}\partial_{xy}^2 - \hat{\mathbf{z}}\partial_{xz}^2] P^N(\mathbf{r}, t), \end{aligned} \quad (34)$$

and the *scalar beam propagator*,  $P^N(\mathbf{r}, t)$ , is given in (31).

### 5. EXAMPLE: PULSED-QUADRATIC FRAMES

The general frame representation in Section 4 is applied here for the special case of pulsed-quadratic windows which has been used extensively for modeling beam propagation, since they maximize the localization as implied by the uncertainty principle, and yield analytically trackable beam-type propagators [4–7, 11, 20]. The pulsed-quadratic synthesis spatial and spectral windows are

$$\check{\psi}(\mathbf{r}_t, t) = \check{f} [t - c^{-1}\Gamma(x^2 + y^2)/2], \tag{35}$$

$$\check{\psi}(\boldsymbol{\kappa}_t, \tau) = -2\pi c\Gamma^{-1}\partial_t^{-1}\check{f} [\tau - c^{-1}(\kappa_x^2 + \kappa_y^2)/(2\Gamma)], \tag{36}$$

where  $\Gamma = \Gamma_r + j\Gamma_j$  is a complex parameter with  $\Gamma_j < 0$ .

In order to evaluate the corresponding pulsed-quadratic analysis window, we shall make use of the high-oversampling approximation (see derivation in the Appendix)

$$\check{\varphi}(\mathbf{r}_t, t) \cong \nu_x\nu_y(S^{-1}\check{\psi})(t), \tag{37}$$

where the operator  $S$  is obtained from  $\check{\psi}$  via

$$S = \int d^2r_t[\psi(\mathbf{r}_t, t) \otimes \psi(\mathbf{r}_t, -t)] \otimes, \quad t \text{ real}, \tag{38}$$

with  $\otimes$  denoting a temporal convolution. For Lorentzian-pulsed quadratic windows the approximation is valid for  $\nu_{x,y} < 0.4$ .

In order to apply the high-oversampling approximation in (37) to the windows in (36) we choose a simple Lorentzian pulse-shape which is attained by choosing the analytic signal

$$\check{f}(t) = \check{\delta} \left( t + \frac{j}{2}T \right), \quad T > 0, \tag{39}$$

where  $T$  is a real parameter which models the time-dependent signal's temporal pulse length and  $\check{\delta}(t)$  is the analytic delta-function in the upper half of the complex  $t$ -plane

$$\check{\delta}(t) = -(j\pi t)^{-1}, \quad \text{Im}t > 0. \tag{40}$$

This signal has a frequency-domain exponential distribution of  $\exp(-T|\omega|/2)$  and therefore its maximal frequency is modeled by  $1/T$ . Next we assume that the window is short on the scale of the aperture field so that  $T \ll \omega_{\max}^{-1}$  where  $\omega_{\max}$  is the EM field maximum frequency in (12). Under this condition, the exponential decay of the frequency-domain window distribution can be neglected over the field effective frequency interval  $\Omega$  and the window can be approximated as constant. Thus the inverse operator

$$S^{-1} \simeq (j\partial_t c^{-1}\Gamma_j/\pi). \tag{41}$$

By inserting approximation (41) into (37) we can approximate the corresponding analysis window by

$$\check{\varphi}(\mathbf{r}_t, t) = (j\nu^2 c^{-1} \Gamma_j / \pi) \check{\delta}'[t - jT/2 - c^{-1} \Gamma(x^2 + y^2)/2], \quad (42)$$

where  $\nu = \nu_x = \nu_y$  is the oversampling parameter in (14) and the prime denotes a derivative with respect to the argument, i.e.,  $\check{\delta}'(t) = 1/j\pi t^2$ .

This type of windows gives rise to pulsed-quadratic beam waveobjects which exhibits frequency independent collimation (Rayleigh) distance and therefore are termed iso-diffracting [46]. The iso-diffracting nature makes these waveobjects highly suitable for UWB radiation representations [2, 5, 10, 43, 47].

The scalar beam propagators are obtained by inserting (36) into (31). The resulting plane-wave spectral integral was evaluated asymptotically in [5, 42]. The resulting paraxial scalar pulsed-beam waveobjects are obtained by utilizing the local beam coordinates,  $\mathbf{r}_b = (x_b, y_b, z_b)$ , which are defined, for a given spectral point  $(\bar{x}, \bar{y}, \bar{\kappa}_x, \bar{\kappa}_y)$  on the frame spectral lattice, by the transformation

$$\begin{bmatrix} x_b \\ y_b \\ z_b \end{bmatrix} = \begin{bmatrix} \cos \bar{\vartheta} \cos \bar{\varphi} & \cos \bar{\vartheta} \sin \bar{\varphi} & -\sin \bar{\vartheta} \\ -\sin \bar{\varphi} & \cos \bar{\varphi} & 0 \\ \sin \bar{\vartheta} \cos \bar{\varphi} & \sin \bar{\vartheta} \sin \bar{\varphi} & \cos \bar{\vartheta} \end{bmatrix} \begin{bmatrix} x - \bar{x}_x \\ y - \bar{x}_y \\ z \end{bmatrix} \quad (43)$$

where  $(\bar{\vartheta}, \bar{\varphi})$  are the spherical angles that define the unit-vector

$$\hat{\boldsymbol{\kappa}} = (\bar{\kappa}_x, \bar{\kappa}_y, \bar{\kappa}_z), \quad \bar{\kappa}_z = \sqrt{1 - \bar{\kappa}_x^2 - \bar{\kappa}_y^2}, \quad (44)$$

i.e.,

$$\cos \bar{\vartheta} = \bar{\kappa}_z, \quad \cos \bar{\varphi} = \bar{\kappa}_x / \sqrt{\bar{\kappa}_x^2 + \bar{\kappa}_y^2}. \quad (45)$$

By utilizing the beam coordinates, the beam waveobject can be evaluated asymptotically by

$$P^N(\mathbf{r}_b, t) \sim \text{Re} \frac{1}{\bar{\kappa}_z} \sqrt{\frac{\Gamma_x(z_b)}{\Gamma_x(0)}} \sqrt{\frac{\Gamma_y(z_b)}{\Gamma_y(0)}} \partial_t^{-1} \check{f} [t - c^{-1} \Psi(\mathbf{r}_b)] \quad (46)$$

$$\Psi(\mathbf{r}_b) = z_b + \frac{1}{2} [\Gamma_x(z_b) x_b^2 + \Gamma_y(z_b) y_b^2],$$

where

$$\Gamma_x(z_b) = 1 / (z_b + \cos^2 \bar{\vartheta} \Gamma^{-1}), \quad \Gamma_y(z_b) = 1 / (z_b + \Gamma^{-1}), \quad (47)$$

are the so-called complex curvatures of the pulsed-beams. Parameterization of the waveobjects in (46) can be found in [5].

Next, the electric field pulsed propagators are evaluated by inserting (46) into (32) and collecting the higher asymptotic order. Alternatively, the asymptotic electric field can be evaluated directly

from (28). Note, that the difference between the electric field spectral integral (28) and the scalar field representation in (31), is only in the *amplitude* elements, so we can sample the amplitude at the on-axis stationary point  $(\kappa_x, \kappa_y) = (\bar{\kappa}_x, \bar{\kappa}_y)$ . Thus, using (45), the electric field  $\mathbf{E}_x^N$  is given by

$$\mathbf{E}_x^N(\mathbf{r}, t) \sim \left( \hat{\mathbf{x}} - \frac{\bar{\kappa}_x}{\bar{\kappa}_z} \hat{\mathbf{z}} \right) \text{Re} \sqrt{\frac{\Gamma_x(z_b)}{\Gamma_x(0)}} \sqrt{\frac{\Gamma_y(z_b)}{\Gamma_y(0)}} \check{f} [t - c^{-1} \Psi(\mathbf{r}_b)], \quad (48)$$

where  $\Gamma_{x,y}(z_b)$  and  $\Psi(\mathbf{r}_b)$  are given in (47) and (46), respectively. The corresponding magnetic field spectral integral may be easily obtained from the electric field by using the well-known relation for plane-waves  $\tilde{\mathbf{H}} = \eta_0^{-1} \hat{\boldsymbol{\kappa}} \times \tilde{\mathbf{E}}$ . By evaluating the resulting spectral integral asymptotically, one obtains

$$\begin{aligned} \mathbf{H}_x^N(\mathbf{r}, t) &= [\bar{\kappa}_x \bar{\kappa}_y \hat{\mathbf{x}} + (\bar{\kappa}_y^2 - 1) \hat{\mathbf{y}} + \bar{\kappa}_y \bar{\kappa}_z \hat{\mathbf{z}}] \\ &\times \frac{-1}{\bar{\kappa}_z \eta_0} \text{Re} \sqrt{\frac{\Gamma_x(z_b)}{\Gamma_x(0)}} \sqrt{\frac{\Gamma_y(z_b)}{\Gamma_y(0)}} \check{f} [t - c^{-1} \Psi(\mathbf{r}_b)], \end{aligned} \quad (49)$$

where  $\eta_0 = \sqrt{\mu_0/\epsilon_0} = 120\pi\Omega$  is the (vacuum) wave impedance. The EM wave components,  $\mathbf{E}_y^N$  and  $\mathbf{H}_y^N$ , can be obtained in a similar manner. The result is

$$\mathbf{E}_y^N(\mathbf{r}, t) \sim \left( \hat{\mathbf{y}} - \frac{\bar{\kappa}_y}{\bar{\kappa}_z} \hat{\mathbf{z}} \right) \text{Re} \sqrt{\frac{\Gamma_x(z_b)}{\Gamma_x(0)}} \sqrt{\frac{\Gamma_y(z_b)}{\Gamma_y(0)}} \check{f} [t - c^{-1} \Psi(\mathbf{r}_b)], \quad (50)$$

and

$$\begin{aligned} \mathbf{H}_y^N(\mathbf{r}, t) &\sim [(\bar{\kappa}_x^2 - 1) \hat{\mathbf{x}} + \bar{\kappa}_x \bar{\kappa}_y \hat{\mathbf{y}} + \bar{\kappa}_x \bar{\kappa}_z \hat{\mathbf{z}}] \\ &\times \frac{1}{\bar{\kappa}_z \eta_0} \text{Re} \sqrt{\frac{\Gamma_x(z_b)}{\Gamma_x(0)}} \sqrt{\frac{\Gamma_y(z_b)}{\Gamma_y(0)}} \check{f} [t - c^{-1} \Psi(\mathbf{r}_b)]. \end{aligned} \quad (51)$$

## 6. CONCLUSION

An exact expansion scheme for time-dependent EM waves in terms of EM pulsed-beams was introduced. By applying a frame-based expansion, the electric and magnetic fields are described as a discrete summation of shifted, tilted and delayed pulsed-beams which emanate from the aperture plane over the frame spectral lattice. The EM propagators are obtained from a scalar propagators by applying simple differential operators. In the short-pulse regime a simple closed form expressions were obtained for the commonly used pulsed-quadratic windows. This EM field expansion is suitable for analyzing EM wave propagation and scattering in complex environments, both in the near and far field regions.

## APPENDIX A. DERIVATION OF (37)

The analysis window can be evaluated by the high-oversampling approximation which, for a time-harmonic frames with frequency  $\omega$ , is given by [47]

$$\|\psi\|^2 \varphi(\mathbf{r}_t, \omega) \cong \nu_x \nu_y \psi(\mathbf{r}_t, \omega). \quad (\text{A1})$$

where  $\psi(\mathbf{r}_t, \omega)$  is the time-harmonic synthesis window and

$$\|\psi\|^2 = \int d^2 r_t \psi(\mathbf{r}_t, \omega) \psi^*(\mathbf{r}_t, \omega). \quad (\text{A2})$$

In order to obtain a time-domain analogue to the approximation in (A1), we apply the inverse (temporal) analytic Fourier transform

$$\check{f}(\mathbf{r}_t, t) = \frac{1}{\pi} \int_0^\infty d\omega f(\mathbf{r}_t, \omega) \exp(j\omega t), \quad (\text{A3})$$

to both sides of (A1). This procedure yields

$$\frac{1}{\pi} \int_0^\infty d\omega \|\psi\|^2 \varphi(\mathbf{r}_t, \omega) \exp(j\omega t) \cong \nu_x \nu_y \check{\psi}(\mathbf{r}_t, t). \quad (\text{A4})$$

Next we use the convolution theorem for analytic signals

$$\frac{1}{\pi} \int_0^\infty d\omega f(\omega) g(\omega) \exp(j\omega t) = f(t) \otimes \check{g}(t), \quad (\text{A5})$$

where  $f$  is a real function,  $\check{g}(t)$  denotes the analytic signal which is corresponding to  $g(\omega)$  and  $\otimes$  denotes temporal convolution. By using (A5) in (A4) we obtain

$$(\text{S}\check{\varphi})(t) \cong \nu_x \nu_y \check{\psi}(\mathbf{r}_t, t), \quad (\text{A6})$$

where the operator

$$\text{S} = \left[ \frac{1}{2\pi} \int d\omega \|\psi\|^2 \exp(j\omega t) \right] \otimes. \quad (\text{A7})$$

Next we insert (A2) into (A7) and invert the order of integrations. This procedure yields

$$\text{S} = \int d^2 r_t \left[ \frac{1}{2\pi} \int d\omega \psi(\mathbf{r}_t, \omega) \psi^*(\mathbf{r}_t, \omega) \exp(j\omega t) \right] \otimes. \quad (\text{A8})$$

Finally by applying the convolution theorem to (A8) we obtain the result in (38) and applying the inverse operator  $\text{S}^{-1}$  to both sides of (A6) yields the result in (37).

## REFERENCES

1. Steinberg, B. Z., E. Heyman, and L. B. Felsen, "Phase space beam summation for time-harmonic radiation from large apertures," *J. Opt. Soc. Am. A*, Vol. 8, 41–59, 1991.
2. Shlivinski, A., E. Heyman, A. Boag, and C. Letrou, "A phase-space beam summation formulation for ultra wideband radiation," *IEEE Trans. Antennas Propagat.*, Vol. 52, 2042–2056, 2004.
3. Chabory, A., S. Bolioli, and J. Sokoloff, "Novel Gabor-based Gaussian beam expansion for curved aperture radiation in dimension two," *Progress In Electromagnetics Research*, Vol. 58, 171–85, 2006.
4. Steinberg, B. Z., E. Heyman, and L. B. Felsen, "Phase space beam summation for time dependent radiation from large apertures: Continuous parametrization," *J. Opt. Soc. Am. A*, Vol. 8, 943–958, 1991.
5. Melamed, T., "Phase-space beam summation: A local spectrum analysis for time-dependent radiation," *Journal of Electromagnetic Waves and Applications*, Vol. 11, No. 6, 739–773, 1997.
6. Shlivinski, A., E. Heyman, and A. Boag, "A pulsed beam summation formulation for short pulse radiation based on windowed radon transform (WRT) frames," *IEEE Trans. Antennas Propagat.*, Vol. 53, 3030–3048, 2005.
7. Melamed, T., "Time-domain phase-space Green's functions for inhomogeneous media," *Ultrawideband/Short Pulse Electromagnetics 6*, E. L. Mokole, M. Kragalott, K. R. Gerlach, M. Kragalott, and K. R. Gerlach (eds.), 56–63, Springer-Verlag, New York, 2007.
8. Shin, S. Y. and L. B. Felsen, "Gaussian beams in anisotropic media," *Applied Phys.*, Vol. 5, 239–250, 1974.
9. Tinkelman, I. and T. Melamed, "Gaussian beam propagation in generic anisotropic wavenumber profiles," *Optics Letters*, Vol. 28, 1081–1083, 2003.
10. Tinkelman, I. and T. Melamed, "Local spectrum analysis of field propagation in anisotropic media, Part I — Time-harmonic fields," *J. Opt. Soc. Am. A*, Vol. 22, 1200–1207, 2005.
11. Tinkelman, I. and T. Melamed, "Local spectrum analysis of field propagation in anisotropic media, Part II — Time-dependent fields," *J. Opt. Soc. Am. A*, Vol. 22, 1208–1215, 2005.
12. Tuz, V. R., "Three-dimensional Gaussian beam scattering from a periodic sequence of bi-isotropic and material layers," *Progress In Electromagnetics Research B*, Vol. 7, 53–73, 2008.

13. Kong, F., B.-I. Wu, H. Huang, J. Huangfu, S. Xi, and J. A. Kong, "Lateral displacement of an electromagnetic beam reflected from a grounded indefinite uniaxial slab," *Progress In Electromagnetics Research*, Vol. 82, 351–366, 2008.
14. Melamed, T. and L. B. Felsen, "Pulsed beam propagation in lossless dispersive media, Part I: Theory," *J. Opt. Soc. Am. A*, Vol. 15, 1268–1276, 1998.
15. Melamed, T. and L. B. Felsen, "Pulsed beam propagation in lossless dispersive media, Part II: A numerical example," *J. Opt. Soc. Am. A*, Vol. 15, 1277–1284, 1998.
16. Melamed, T. and L. B. Felsen, "Pulsed beam propagation in dispersive media via pulsed plane wave spectral decomposition," *IEEE Trans. Antennas Propagat.*, Vol. 48, 901–908, 2000.
17. Kiselev, A. P., "Localized light waves: Paraxial and exact solutions of the wave equation (a review)," *Opt. Spectrosc.*, Vol. 102, 603–622, 2007.
18. Červený, V., M. M. Popov, and I. Pšenčík, "Computation of wave fields in inhomogeneous media — Gaussian beam approach," *Geophys. J. Roy. Astro. Soc.*, Vol. 70, 109–128, 1982.
19. Wu, Z. and L. Guo, "Electromagnetic scattering from a multilayered cylinder arbitrarily located in a Gaussian beam, a new recursive algorithms," *Progress In Electromagnetics Research*, Vol. 18, 317–333, 1998.
20. Heyman, E., "Pulsed beam propagation in an inhomogeneous medium," *IEEE Trans. Antennas Propagat.*, Vol. 42, 311–319, 1994.
21. Melamed, T., "Phase-space Green's functions for modeling time-harmonic scattering from smooth inhomogeneous objects," *J. Math. Phys.*, Vol. 46, 2232–2246, 2004.
22. Hadad, Y. and T. Melamed, "Tilted Gaussian beam propagation in inhomogeneous media," *J. Opt. Soc. Am. A*, Vol. 27, 1840–1850, 2010.
23. Melamed, T., E. Heyman, and L. B. Felsen, "Local spectral analysis of short-pulse-excited scattering from weakly inhomogeneous media: Part I — forward scattering," *IEEE Trans. Antennas Propagat.*, Vol. 47, 1208–1217, 1999.
24. Melamed, T., E. Heyman, and L. B. Felsen, "Local spectral analysis of short-pulse-excited scattering from weakly inhomogeneous media: Part II — Inverse scattering," *IEEE Trans. Antennas Propagat.*, Vol. 47, 1218–1227, 1999.
25. Galdi, V., H. Feng, D. A. Castanon, W. C. Karl, and L. B. Felsen,

- “Moderately rough surface underground imaging via short-pulse quasi-ray Gaussian beams,” *IEEE Trans. Antennas Propagat.*, Vol. 51, 2304–2318, 2003.
26. Melamed, T., “On localization aspects of frequency-domain scattering from low-contrast objects,” *IEEE Antennas Wirel. Propag. Lett.*, Vol. 2, 40–42, 2003.
  27. Wang, M.-J., Z.-S. Wu, Y.-L. Li, and G. Zhang, “High resolution range profile identifying simulation of laser radar based on pulse beam scattering characteristics of targets,” *Progress In Electromagnetics Research*, Vol. 96, 193–204, 2009.
  28. Lim, S.-H., J.-H. Han, S.-Y. Kim, and N.-H. Myung, “Azimuth beam pattern synthesis for airborne SAR system optimization,” *Progress In Electromagnetics Research*, Vol. 106, 295–309, 2010.
  29. Collin, R. E., “Scattering of an incident Gaussian beam by a perfectly conducting rough surface,” *IEEE Trans. Antennas Propagat.*, Vol. 42, 70–74, 1994.
  30. Kilic, O. and R. H. Lang, “Scattering of a pulsed beam by a random medium over ground,” *Journal of Electromagnetic Waves and Applications*, Vol. 15, No. 4, 481–516, 2001.
  31. Hoppe, D. J. and Y. Rahmat-Samii, “Gaussian beam reflection at a dielectric-chiral interface,” *Journal of Electromagnetic Waves and Applications*, Vol. 6, No. 1–6, 603–624, 1992.
  32. Wang, M.-J., Z.-S. Wu, and Y.-L. Li, “Investigation on the scattering characteristics of Gaussian beam from two dimensional dielectric rough surfaces based on the Kirchhoff approximation,” *Progress In Electromagnetics Research B*, Vol. 4, 223–235, 2008.
  33. Sakurai, H. and S. Kozaki, “Scattering of a Gaussian beam by a radially inhomogeneous dielectric sphere,” *Journal of Electromagnetic Waves and Applications*, Vol. 15, 1673–1693, 2001.
  34. Falco, F. and T. Tamir, “Improved analysis of nonspecular phenomena in beams reflected from stratified media,” *J. Opt. Soc. Am. A*, Vol. 7, 185–190, 1990.
  35. Bass, F. and L. Resnick, “Wave beam propagation in layered media,” *Progress In Electromagnetics Research*, Vol. 38, 111–123, 2002.
  36. Kong, J. A., “Electromagnetic wave interaction with stratified negative isotropic media,” *Journal of Electromagnetic Waves and Applications*, Vol. 15, No. 10, 1319–1320, 2001.
  37. Hadad, Y. and T. Melamed, “Non-orthogonal domain parabolic equation and its Gaussian beam solutions,” *IEEE Trans.*

- Antennas Propagat.*, Vol. 58, 1164–1172, 2010.
38. Hadad, Y. and T. Melamed, “Parameterization of the tilted Gaussian beam waveobjects,” *Progress In Electromagnetics Research*, Vol. 102, 65–80, 2010.
  39. Chou, H.-T., P. H. Pathak, and R. J. Burkholder, “Application of Gaussian-ray basis functions for the rapid analysis of electromagnetic radiation from reflector antennas,” *IEE Proc., Microw. Antennas Propag.*, Vol. 150, 177–183, 2003.
  40. Chou, H.-T., P. H. Pathak, and R. J. Burkholder, “Novel Gaussian beam method for the rapid analysis of large reflector antennas,” *IEEE Trans. Antennas Propagat.*, Vol. 49, 880–893, 2001.
  41. Chou, H.-T. and P. H. Pathak, “Fast Gaussian beam based synthesis of shaped reflector antennas for contoured beam applications,” *IEE Proc., Microw. Antennas Propag.*, Vol. 151, 13–20, 2004.
  42. Melamed, T., “Exact beam decomposition of time-harmonic electromagnetic waves,” *Journal of Electromagnetic Waves and Applications*, Vol. 23, No. 8–9, 975–986, 2009.
  43. Melamed, T., “TE and TM beam decomposition of time-harmonic electromagnetic waves,” *J. Opt. Soc. Am. A*, Vol. 28, 401–409, 2011.
  44. Heyman, E. and T. Melamed, “Space-time representation of ultra wideband signals,” *Advances in Imaging and Electron Physics*, Vol. 103, 1–63, Elsevier, 1998.
  45. Steinberg, B. Z. and E. Heyman, “Phase space beam summation for time dependent radiation from large apertures: Discretized parametrization,” *J. Opt. Soc. Am. A*, Vol. 8, 959–966, 1991.
  46. Heyman, E. and T. Melamed, “Certain considerations in aperture synthesis of ultrawideband/short-pulse radiation,” *IEEE Trans. Antennas Propagat.*, Vol. 42, 518–525, 1994.
  47. Shlivinski, A., E. Heyman, and A. Boag, “A phase-space beam summation formulation for ultrawide-band radiation — Part II: A multiband scheme,” *IEEE Trans. Antennas Propagat.*, Vol. 53, 948–957, 2005.